Environmental Science Advances

ROYAL SOCIETY OF CHEMISTRY

PAPER

View Article Online
View Journal | View Issue

Cite this: *Environ. Sci.: Adv.*, 2026, **5**, 1106

Oxidation of TcO_2 and UO_2 by aqueous Mn(III)-citrate and Mn(III)-tartrate under anoxic conditions: implications for technetium and uranium fate and transport

Zachary Murphy, Zachary Ronchetti, Cassandra Munoz, David Rai, II and Vasileios Anagnostopoulos *

There are several United States Department of Energy (DOE) sites that have been dealing with the problem of legacy nuclear waste in the environment for many generations. Two major risk-driving radionuclides in this legacy waste are uranium and technetium-99. Due to their radioactivity, the increase in concentration of these radionuclides in the environment represents a significant concern to environmental health and safety. Uranium and technetium both have increased solubility and mobility in the environment when oxidized from U(IV) to U(VI) and from Tc(IV) to Tc(VII), respectively. This project investigated the role of Mn(III)-tartrate and Mn(III)-citrate in influencing the redox behavior and stability of uranium, from uranium dioxide (UO_2), and technetium, from technetium oxide (TcO_2). For each radionuclide, anaerobic batch kinetic experiments of UO_2 and TcO_2 in the presence of these Mn(III)-ligands were conducted at pH 8 and 10, and the radionuclide concentration in the aqueous phase was monitored over time. Both the Mn(III)-tartrate and Mn(III)-citrate complexes effectively induced dissolution of uranium and technetium, however, differences were seen with increasing ligand concentration and pH. Higher concentrations of the Mn(III)-ligand complexes resulted in higher concentrations of aqueous uranium or technetium over time, supporting Mn(III) induced oxidation of these radionuclides. Additionally, the Mn(III)-tartrate complex resulted in more oxidation at pH 8 for both uranium and technetium while the Mn(III)-citrate ligand provided more oxidation at pH 10 for uranium and was comparable for technetium. The data presented in this study is useful for creating expected uranium and technetium transport models based on the abundance of naturally occurring manganese species.

Received 11th August 2025
Accepted 25th February 2026

DOI: 10.1039/d5va00264h

rsc.li/esadvances

Environmental significance

The presence of legacy nuclear waste, specifically uranium and technetium-99, from sites like those managed by the Department of Energy (DOE), poses a significant environmental risk due to its radioactivity. These radionuclides become highly mobile and soluble when oxidized from their less mobile forms (U(IV) to U(VI) and Tc(IV) to Tc(VII)). This study's environmental significance lies in demonstrating that naturally occurring Mn(III)-ligand complexes, such as Mn(III)-citrate and Mn(III)-tartrate, can effectively induce the oxidation and dissolution of uranium dioxide (UO_2) and technetium oxide (TcO_2) even under anoxic conditions, where they are expected to be immobile. Understanding how these common manganese species influence radionuclide redox behavior and stability is crucial for predicting the spread of contamination and inform remediation strategies.

1. Introduction

The presence of legacy nuclear waste in the environment has been a problem in the United States since the mid-20th century. A majority of this waste originates from World War II and the Cold War as a byproduct of nuclear weapons development and testing.[1,2] As this was over 70 years ago, during the infancy of the U.S. nuclear program as well as during active war times, the understanding of radioactive waste management and its environmental impact was limited. As a result, large quantities of radioactive waste were improperly contained, including the release of waste into trenches and ponds under the assumption that the waste would evaporate, preventing further harm.[2,3] While most waste was placed in underground storage tanks, these were only designed to last a few decades until permanent disposal solutions were developed.[4] With the passage of time, however, many of these tanks have leaked, releasing additional radioactive material into the environment.[5–7] Two major risk-driving radionuclides in this legacy waste are uranium, with several radioactive isotopes, and technetium-99.[8]

Department of Chemistry, University of Central Florida, Orlando, FL, 32816, USA. E-mail: Vasileios.Anagnos@ucf.edu

Uranium is a primary component of nuclear waste and a significant source of environmental contamination.[8,9] Uranium dioxide (UO_2), an insoluble U(IV) mineral, is the dominant uranium phase in spent nuclear fuel and forms a major component of uranium mill tailings.[10] Uranium contamination can arise from the corrosion of spent nuclear fuel, improperly managed nuclear waste, and uranium mill tailings, all of which can leach uranium into groundwater over time.[5,11,12] Once released in the environment, the fate and transport of uranium are governed by multiple pathways, including sorption, ligand complexation, plant uptake, biogenic interactions, and colloidal formation.[13–19] Understanding these processes is essential for modeling uranium behavior and predicting long-term environmental impact. One critical factor influencing uranium mobility is its oxidation state. While U(IV) is typically insoluble, U(VI) species, such as the uranyl ion, UO_2^{2+}, are highly soluble and mobile.[20,21] As such, remediation strategies addressing the biogenic reduction of uranium have been proposed.[22,23] Therefore, conditions that promote the oxidation of U(IV) to U(VI) must be carefully studied to assess the extent of contamination at legacy sites and to inform models for long-term waste storage in geological repositories.

Technetium is a byproduct of uranium fission, with a yield of approximately 6%.[2] It is of great concern that technetium has infiltrated the environment as its half-life of approximately 2.13×10^5 years is short enough to give it a significant contribution to total activity at contaminated sites, but long enough that it will persist for the foreseeable future.[2] Like uranium, technetium's fate and transport are also governed by its oxidation state. Under oxidizing conditions, technetium exists as Tc(VII) – commonly the aqueous pertechnetate anion, TcO_4^-. Due to its negative charge, TcO_4^- generally does not sorb onto soil or mineral surfaces and is therefore highly environmentally mobile.[2,24] When reduced to Tc(IV), technetium precipitates as an amorphous solid, TcO_2, and has very low solubility, making it environmentally immobile. The environmental immobility of TcO_2 and expected stability in suboxic and anoxic environments has led to the proposition of reductive conversion of TcO_4^- to TcO_2 as a strategy for environmental remediation of technitium.[25–30] It has since been discovered, however, that TcO_2 and UO_2 are susceptible to reoxidation by naturally occurring oxidants, even in anoxic conditions, by geochemically relevant oxidizing agents.[31–33] This includes Mn(III)-ligand complexes, such as Mn(III)-pyrophosphate.[34,35] This study further expands on this phenomenon by investigating the oxidative effects of other Mn(III)-ligand complexes due to the oxidizing potential of Mn(III) and high solubility of these complexes.[36]

Manganese is a naturally occurring element that is widely present in soil, water, and rocks. Manganese oxides are of particular interest as they are widely present in both terrestrial and aquatic environments, most often appearing in soils and sediments.[37] While Mn(III) is known to be a strong oxidant, its relevance has long been overlooked because of its tendency to rapidly disproportionate into Mn(II) and Mn(IV).[38] However, it has since been discovered that Mn(III) can be stabilized by naturally occurring ligands during enzymatic oxidation of Mn(II) to Mn(IV).[38] Select Mn(III)-ligand complexes have been investigated for the redox properties.[39,40] Mn(III)-ligand complexes have been detected in suboxic and anoxic waters, but the specific ligands responsible for Mn(III) stabilization in these conditions remain largely unidentified.[41] Citrate and tartrate, which are commonly found in the environment and utilized by bacteria, are potential candidates for Mn(III) complexation and were therefore selected for investigation in this study.[42]

Previous research has demonstrated that Mn(III)-ligand complexes are highly pH sensitive.[39,43] Below pH 8, Mn(III)-citrate and Mn(III)-tartrate become increasingly unstable and are prone to dissociation and reduction to Mn(II).[40] While the manganese oxidation capacity of microbial activity is generally higher under acidic conditions, recent studies have shown that certain strains can still induce manganese oxidation up to pH 10.[44] Additionally, sites with nuclear waste contamination can also cause highly alkaline conditions due to a combination of the waste material itself and the impact of cementitious barriers.[45,46] Understanding the pH dependence of Mn(III)-ligand stability is therefore critical for evaluating their potential to oxidize UO_2 and TcO_2 in the environment.

While Mn(III) has been recognized as a potential oxidant capable of remobilizing reduced radionuclide phases under anoxic conditions, most experimental studies have focused on Mn(III) stabilized by strong inorganic or synthetic ligands, such as pyrophosphate or EDTA.[34,35,39,47] These ligands, while effective at maintaining Mn(III) in solution, may not be representative of the organic ligands that dominate many natural and engineered subsurface environments. In contrast, low-molecular weight organic acids such as citrate and tartrate are commonly produced by microbial activity, are abundant in soils and sediments, and participate actively in metal complexation and redox cycling.[42] Despite their environmental relevance, the ability of Mn(III)-organic acid complexes to oxidize reduced uranium and technetium phases under alkaline, anoxic conditions remains poorly studied. Addressing these gaps is critical for accurately assessing the long-term stability of reduced U and Tc phases in contaminated environments.

Give these knowledge gaps, the objective of this study was to evaluate and quantify the oxidative dissolution of UO_2 and TcO_2 by soluble Mn(III)-citrate and Mn(III)-tartrate. The effects of ligand identity (citrate and tartrate), pH, and ligand concentration on Mn(III) reactivity were assessed to broaden the understanding of the radionuclide geochemical fate and transport. Insights gained from these reactions will enhance radionuclide transport models, predicting the potential spread of contamination in the environment. Additionally, these findings may inform the behavior of other redox-active radionuclides and contaminants that could undergo Mn-mediated oxidation, contributing to their increased mobility and environmental persistence.

2. Experimental

2.1 UO_2 synthesis

The synthesis of uranium dioxide was developed from existing literature.[48] A mass of 200 mg of uranyl nitrate (Certified ACS, Fisher Chemical) was dissolved in 10 mL of ultra-pure water

(18.2 MΩ cm, Barnstead Nanopure). While stirring the uranyl nitrate solution, 10 mL of acetone (ACS Grade, Fisher Chemical) was added. After 10 minutes, 10 mL of diethylene glycol (99%, Thermo Scientific) was combined with the solution. It was then mixed for two hours, then transferred to a PTFE lined hydrothermal autoclave reactor and heated at 215 °C for three days. Once cooled, the precipitate was collected *via* centrifugation and washed with ultra-pure water and ethanol (99.5+%, Acros Organics) until the supernatant ran clear. The remaining precipitate was dried at 50 °C overnight in a conventional oven. XRD (Empyrean, PANalytical) was run using a 1.8 kW copper X-ray tube (1.54 Å) from 2θ of 20° to 70° for product confirmation.

2.2 TcO_2 synthesis

The TcO_2 solid was synthesized from a NH_4TcO_4 stock (Oak Ridge National Laboratory) following a method adapted from Stanberry, *et al.*[34] Synthesis was performed inside of an anaerobic glovebox (I-Lab, Inert) using ultra-high purity nitrogen (99.999%, Aigas), with 1.5 mL microcentrifuge tubes acting as the reaction vessels and $Na_2S_2O_4$ used in excess as a reducing agent. For each sample, a 1 mL solution of 1.75 mM NH_4TcO_4, 160 mM $Na_2S_2O_4$ (85%+, ACROS Organics), and 150 mM NaOH (Laboratory Grade, Fisher Chemical) was prepared and matured for at least 24 hours. Each sample was then washed five times with ultra-pure water to remove dithionite from the solid, centrifuging (Mini 10K, Huyanu) at 10 000 rpm for 10 minutes to remove the supernatant. The solid was left in a minimal amount of water until it was used for experimentation. The supernatant was collected and analyzed with liquid scintillation counting (LSC, AccuFLEX LSC-8000, Hitachi) to track any technetium that may have been extracted during the washing process. The limit of detection (LoD) and limit of quantification (LoQ) for Tc with LSC are 176 pM and 238 pM, respectively.

2.3 Mn(III)-ligand complex synthesis

The Mn(III)-ligand complex stocks were synthesized outside of the glovebox, following a method derived from Kostka, *et al.*[47] For both Mn(III)-citrate and Mn(III)-tartrate, sodium citrate dihydrate (>98%, Fisher Chemical) or potassium sodium L-(+)-tartrate tetrahydrate (>98%, Tokyo Chemical Industry), respectively, was dissolved in ultra-pure water with moderate heat and stirring to make a 250 mM ligand stock. The solution was adjusted to pH 9 using NaOH and HCl (Laboratory Grade, Fisher Chemical). Mn(III) acetate dihydrate (98%, Acros Organics) was added slowly to make a 5 mM solution of Mn(III), making sure to maintain pH 9 during addition. Once completely dissolved, the heat was removed, and the solution was allowed to stir overnight. The solution was then filtered with a 0.2 μm polyethersulfone (PES) membrane filter to remove any potential MnO_2 particulates and pH adjusted to pH 8 or 10 based on the desired experimental condition. The stock was then brought to the target stock volume, degassed to remove any dissolved oxygen, and brought into an anaerobic glovebox where it was allowed to equilibrate for at least 24 hours. The final concentration of the Mn(III)-ligand complex stocks were confirmed before experimentation using leucoberbelin blue as described below.

2.4 Mn(III) quantification using leucoberbelin blue method

The concentration of Mn(III) in the Mn(III)-ligand stocks and batch kinetic samples was measured using leucoberbelin blue (LBB) as described in literature.[49] The absorbance of the samples was measured at 624 nm, and a calibration curve was prepared with potassium permanganate (99.0%, Beantown Chemical) at 0.2 mM LBB (65% dye content, Sigma-Aldrich). The difference in electron transfer from Mn(VII) in potassium permanganate and Mn(III) in the samples was accounted for in the calibration, and an equivalent of 1–20 μM Mn(III) was used in the calibration curve. The potassium permanganate stock was standardized *via* titration with sodium oxalate (99%, Alpha Aesar) to account for degradation over time.

2.5 Job plots

The manganese-to-ligand ratio in the Mn(III)-citrate and Mn(III)-tartrate complexes was studied using the method of continuous variation (Job plot). For each complex, a series of solutions was prepared where the total combined concentration of Mn(III) and ligand was maintained at 10 mM, while the mole fraction of ligand was varied between 0.1 to 0.9. To prepare each mixture, appropriate amounts of manganese(III) acetate dihydrate (98%, Acros Organics) and a 10 mM ligand stock solution were combined in a 50 mL centrifuge tube to match the desired mole fraction and maintain a total metal + ligand concentration of 10 mM. While adding the manganese(III) acetate, the pH was continually adjusted with NaOH and HCl to maintain the desired pH. The solutions were then diluted to 50 mL with ultra-pure water. Solutions were rotated overnight, after which the pH was readjusted as needed. The absorbance of each solution was measured at 430 nm for Mn(III)-citrate and 472 nm for Mn(III)-tartrate to monitor the effective Mn(III)-ligand concentration. Direct absorbance was used in place of the LBB method of quantifying exact total Mn(III) concentrations since no significant difference was found between the calculation of the ligand mol fraction from these two methods. Job plots were then constructed by plotting absorbance as a function of ligand mole fraction. This process was repeated at pH values from 8.0 to 9.5 in 0.5-unit increments. The mole fraction corresponding to the maximum absorbance at each pH was calculated and used to examine pH-dependent trends in complex formation and variations in Mn(III) complexation with citrate and tartrate.

2.6 Batch kinetic experiments

For the purpose of simulating an oxygen-free environment, all experiments were performed in an anaerobic glovebox that was kept below 0.1 ppm of O_2. All batch kinetic dissolution experiments were performed in triplicate. Batch dissolution studies were conducted using 18.5 μmol of solid UO_2 in 10 mL of the desired solution composition or 1.75 μmol of washed Tc(IV) in 12 mL of the desired solution composition in 15 mL test tubes. Experiments were conducted at 1 to 3 mM of the Mn(III)-ligand complexes. Molar ratios of U(IV) : Mn(III) were tested at 1 : 0.54 and 1 : 1.62, while molar ratios of Tc(IV) : Mn(III) were tested at 1 : 8.57 and 1 : 17.1. The pH was adjusted using HCl and NaOH, and

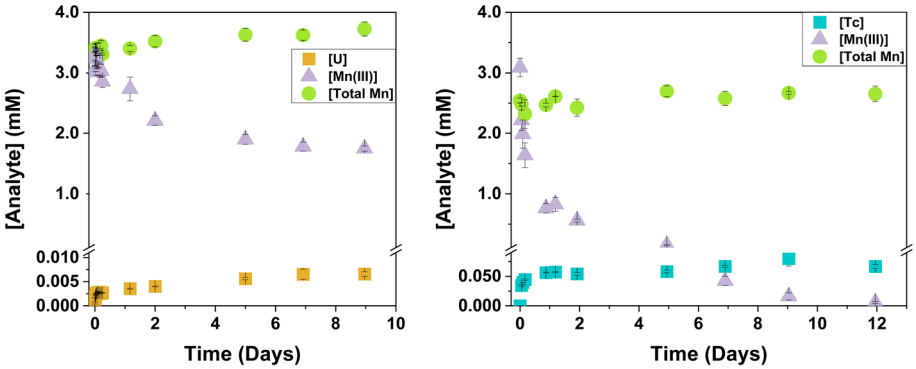

Fig. 1 Kinetic dissolution trials of UO_2 (left) and TcO_2 (right) with 3 mM Mn(III)-tartrate at pH 10 showing the aqueous concentrations of U, Tc, Mn(III) and total manganese over time.

regulated to pH 8 or 10 since the ligand complex is known to degrade beyond this range. Aliquots of the sample were removed and filtered with a 0.22 μm PTFE filter over a span of up to 2 weeks and analyzed for aqueous Mn(III) using LBB as described above, total aqueous manganese and uranium using ICP-MS, and/or aqueous technetium concentrations using LSC. Control experiments for UO_2 and TcO_2 were first conducted in water in the absence of any Mn or ligand, then also conducted in the presence of free ligand and the absence of Mn to account for any ligand assisted dissolution. The control data used in the results figures are from the latter of these two control experiments, as this would account for the largest amount of non-oxidative dissolution of UO_2 and TcO_2. Control experiments for the Mn(III)-ligand complexes were conducted at 3 mM Mn(III)-ligand in the absence of any solid phase to consider Mn(III) and total aqueous manganese loss *via* alternative mechanisms.

2.7 Inductively coupled plasma-mass spectrometry (ICP-MS)

Total uranium and manganese concentrations in the batch kinetic trials were monitored using ICP-MS (iCAP RQ, Thermoscientific). Samples were prepared in 2% nitric acid (Trace Metal Grade, Fisher Chemical). Instrumental drift was accounted for and corrected with the use of the internal standards In, Re, Sc, Tb, and Ge. The instrument utilized kinetic energy discrimination (KED) to eliminate diatomic interferences. The LoD and LoQ for uranium are 0.79 pM and 2.4 pM, and for manganese are 11.3 pM and 34.3 pM, respectively.

3. Results

3.1 Mn(III)-citrate and Mn(III)-tartrate stability

The stability of Mn(III)-citrate and Mn(III)-tartrate was first examined in the absence of any mineral phases. There is no available literature that addresses the direct measurement of formation constants for Mn(III)-citrate and Mn(III)-tartrate. Experimentally, in 3 mM solutions of the respective Mn(III)-ligand complexes, significant loss of Mn(III) was observed over time. Mn(III)-citrate was found to be more stable at pH 8, while Mn(III)-tartrate showed greater stability at pH 10. Although Mn(III) loss could initially be attributed to the disproportionation of manganese, this process would result in the formation and precipitation of Mn(IV). However, ICP-MS analysis showed that the total aqueous manganese concentration remained constant over time, inconsistent with Mn(IV) precipitation. Additionally, solid-phase characterization from the uranium dioxide dissolution experiments showed no evidence of manganese precipitation (SI). As such, the observed Mn(III) loss is attributed to ligand-mediated electron transfer, in which the ligand reduces Mn(III) to Mn(II), maintaining the total manganese concentration in solution and preventing Mn(IV) precipitation.[39,43] Although no studies have been conducted to directly characterize this oxidized ligand, the single electron transfer from Mn(III) would then likely form radical species from the oxidized ligand, which may also contribute to the oxidation of UO_2 or TcO_2 conducted in this study.[39,43]

The example kinetic curves (Fig. 1) are specific to one set of parameters, 3 mM of Mn(III)-tartrate at pH 10, but illustrate the general trends seen amongst the rest of the trials as well. The given radionuclide, U or Tc, has a relatively rapid increase before dissolution slows and then plateaus. Inversely, the Mn(III) concentration has a relatively rapid decline before consumption slows and then plateaus. In the case of the technetium trials, the Mn(III) was entirely consumed and thus the plateau occurs at zero mM. These kinetics do not follow pseudo-zero, pseudo-first, or pseudo-second order reactions.

Due to the instability of the Mn(III)-ligand complex, the amount of Mn(III) reduction and uranium or technetium oxidation is not expected to follow the anticipated ratios, based on the general scheme reactions shown below:

$$2\text{Mn(III)-L} + UO_2 \rightarrow 2\text{Mn(II)-L}^- + UO_2^{2+} \quad (1)$$

$$3\text{Mn(III)-L} + TcO_2 + 2H_2O \rightarrow 3\text{Mn(II)-L}^- + TcO_4^- + 4H^+ \quad (2)$$

The additional pathways for Mn(III) reduction provided by the ligands presents a complex system in which kinetic models would require the differentiation of Mn(II) production *via* electron transfer from the ligand or from the minerals present. Additionally, contributions to Mn(III) consumption for the technetium trials may be due to the presence of technetium sulfides. It is noted in Stanberry *et al.*, which utilizes

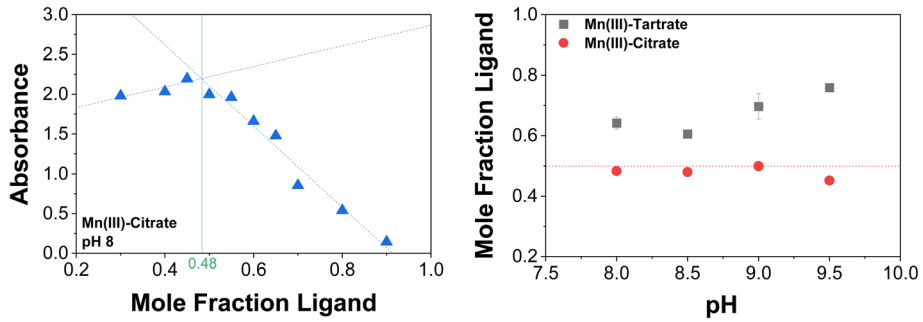

Fig. 2 Example Job plot of Mn(III)-citrate at pH 8, showing the absorbance at 430 nm as a function of the mole fraction of ligand (left). The mole fraction at which corresponds to the point of maximum absorbance represents the mole fraction ratio in the Mn(III)-citrate complex at this pH. The relationship between the mole fraction of ligand and pH is also shown (right) for Mn(III)-citrate (red circle) and Mn(III)-tartrate (gray square) from pH 8 to 9.5. A horizontal line at a mole fraction of ligand of 0.5 is present in red for reference.

the same method of TcO_2 solid synthesis, that technetium sulfides are thought to be present and contributing to the increased consumption of Mn(III) beyond the expected 3 : 1 ratio.[34] This increased consumption of Mn(III) for the technetium trials is thus suspected to be due to a combination of these factors.

To better understand the behavior of Mn(III)-ligand complexes, further studies of Mn(III)-citrate and Mn(III)-tartrate were performed. Job plots were utilized to determine the manganese : ligand ratio at pH 8.0 to 9.5. These results are summarized in Fig. 2, which shows the ligand mole fraction as a function of pH. For Mn(III)-citrate, the citrate mole fraction remained relatively constant around 0.5, consistent with the formation of a 1 : 1 Mn(III) : citrate complex. This stoichiometry is consistent with prior aqueous speciation and kinetic studies that Mn(III)-citrate as a predominantly 1 : 1 complex in solution under circumneutral to mildly basic conditions.[39,43] This is reasonable, as citrate has a −3 charge in this pH range and can effectively charge-balance the Mn(III) cation. In contrast, the mole fraction of tartrate in Mn(III)-tartrate ranged from approximately 0.60 to 0.75, with a slight increase at higher pH. This suggests the presence of Mn(III)-tartrate complexes with a higher ligand-to-metal ratio. A charge balanced complex such as $Mn(III)_2tartrate_3$ would have a mole fraction of ligand of 0.6, which may represent the dominant species near pH 8. Complexes with an even larger excess of ligand seem to predominate for Mn(III)-tartrate at higher pH. The authors have found no applicable literature addressing Mn(III)-tartrate stoichiometry, and attempts to further investigate the complexes using ^{1}H-NMR were inconclusive due to signal overlap with H_2O and were not pursued further (SI).

3.2 UO_2 dissolution

The UO_2 used in these trials was shown to be stable in water over the period of these studies. This is consistent with previous findings demonstrating that the synthesized UO_2 remained stable in water for up to 50 days.[48] Control experiments with UO_2 in the presence of citrate or tartrate without Mn(III) showed minor uranium release into the aqueous phase, attributed to ligand-assisted dissolution. In trials with Mn(III)-citrate at pH 8, a similar extent of uranium dissolution was observed, indicating that little to no UO_2 oxidation occurred under these conditions. However, at pH 10, the uranium dissolution was magnified in the presence of Mn(III)-citrate, providing evidence that these complexes are capable of oxidizing UO_2 under more alkaline conditions. The Pourbaix diagram of uranium under these experimental conditions (SI) shows a higher redox potential needed to oxidize uranium at pH 8 than at pH 10. Additionally, given that the loss of Mn(III) in the Mn(III)-citrate complex was higher at pH 10 even in the absence of UO_2, there

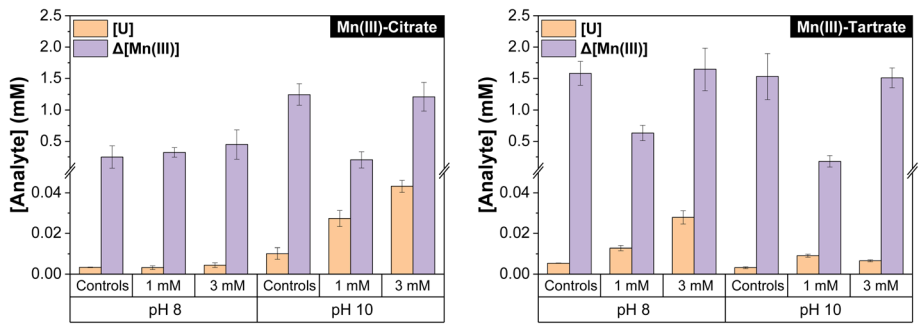

Fig. 3 Final aqueous uranium concentration (orange) and change in aqueous Mn(III) concentration (purple) from UO_2 oxidation with Mn(III)-citrate (left) and Mn(III)-tartrate (right). Control experiments show the dissolution of UO_2 with ligand in the absence of Mn, and the stability of the 3 mM Mn(III)-ligand complex in the absence of UO_2.

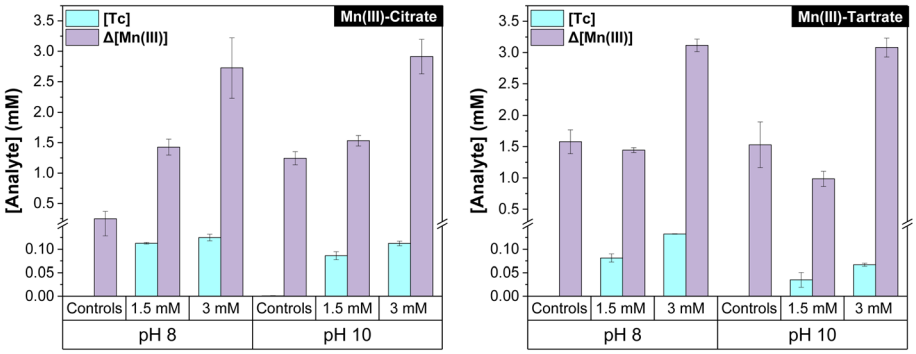

Fig. 4 Final aqueous technetium concentration (blue) and change in aqueous Mn(III) concentration (purple) from TcO_2 oxidation with Mn(III)-citrate (left) and Mn(III)-tartrate (right). Control experiments show the dissolution of TcO_2 with ligand in the absence of Mn, and the stability of the 3 mM Mn(III)-ligand complex in the absence of TcO_2.

was likely a higher number of radicals being formed at pH 10 due to the electron exchange between Mn(III) and citrate. This higher concentration of radical species might contribute more significantly to the oxidation of UO_2, causing the higher amount of UO_2 oxidation at pH 10 with Mn(III)-citrate. The loss of Mn(III) observed in the citrate trials did not differ significantly between control and UO_2-containing systems, which is consistent with the low concentration of uranium oxidized relative to the excess Mn(III) present (Fig. 3).

Mn(III)-tartrate showed minimal impact on UO_2 dissolution at pH 10, but increased aqueous uranium concentrations at pH 8, in contrast to the behavior observed with Mn(III)-citrate. The loss of Mn(III) in the control experiments was comparable for Mn(III)-tartrate at both pH 8 and 10, indicating comparable radical activity from the oxidation of tartrate across the pH range of this study. The increase in uranium oxidation at pH 8 could then be due to differences in the Mn(III)-tartrate speciation. As previously discussed, Job plots indicate that Mn(III)-citrate forms a 1 : 1 metal-to-ligand complex, while Mn(III)-tartrate forms multi-ligand complexes, with an increasing metal-to-ligand ratio at higher pH. The presence of additional tartrate ligands at elevated pH may result in steric hindrance, reducing the ability of the complex to interact with and oxidize the UO_2 surface. As with the citrate trials, Mn(III) degradation in the tartrate systems was comparable between control and UO_2-containing experiments, consistent with the limited extent of UO_2 oxidation observed.

Post-dissolution characterization of the residual solid phase using DLS, SEM, and XRD confirmed that the hydrodynamic radius, particle distribution, and crystal structure remained consistent with the pre-dissolution UO_2 (SI). These results indicate that UO_2 remained the dominant solid phase throughout the kinetic trials, with no evidence of manganese precipitation as discussed earlier.

Overall, while both Mn(III)-citrate and tartrate exhibit the capacity to oxidize UO_2, the extent of uranium release is relatively minor compared to the total 1.85 mM uranium present in the system and the excess Mn(III) available. In comparison, literature reports involving Mn(III)-pyrophosphate show more pronounced UO_2 oxidation, likely due in part to differences in UO_2 synthesis methods and the greater oxidation resistance of the UO_2 particles used in this study.[35] Additional studies have been conducted on environmentally relevant oxidizing agents which show that UO_2 oxidation also occurs in the presence of iron (hydr)oxides and manganese (hydr)oxides.[31,50,51] While formal kinetic rate constants were not measured in the present work, the extent of oxidation observed over similar experimental timeframes suggests that UO_2 oxidation proceeds comparably in these systems.

3.3 TcO_2 dissolution

The TcO_2 used in these trials was shown to be resistant to dissolution by the free ligands when in the absence of Mn(III). This indicates that there was no ligand assisted dissolution and thus tests of the TcO_2 solid in water were not necessary. In trials with Mn(III)-citrate, considerable dissolution was seen at both pH 8 and 10, although marginally higher at pH 8. At both pHs there was slightly more dissolution with the higher

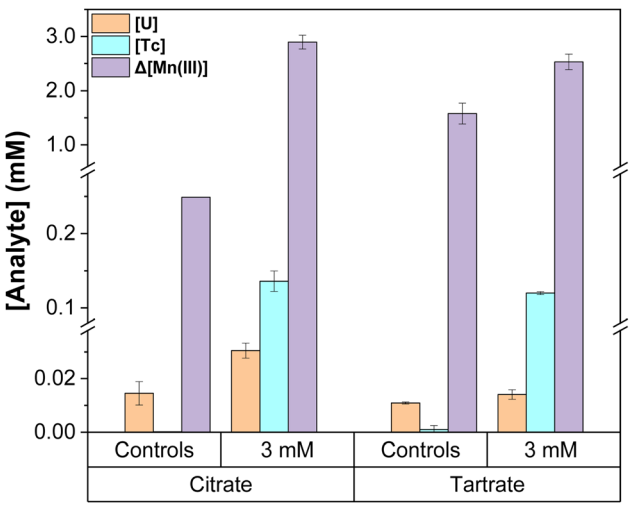

Fig. 5 Final aqueous uranium concentration (orange), technetium concentration (blue) and change in aqueous Mn(III) concentration (purple) from UO_2 and TcO_2 combined oxidation with Mn(III)-citrate and Mn(III)-tartrate at pH 8. Control experiments show the dissolution of UO_2 and TcO_2 with ligand in the absence of Mn, and the stability of the Mn(III)-ligand complex in the absence of UO_2 or TcO_2.

Table 1 Summary of final concentrations of U and Tc after dissolution at pH 8

Solution	Radionuclide (s)	[U] (mM)	[Tc] (mM)
3 mM Mn(III)-citrate	UO_2	0.0044 ± 0.001	—
3 mM Mn(III)-tartrate	UO_2	0.0279 ± 0.003	—
3 mM Mn(III)-citrate	TcO_2	—	0.125 ± 0.007
3 mM Mn(III)-tartrate	TcO_2	—	0.133 ± 0.0006
3 mM Mn(III)-citrate	UO_2 and TcO_2	0.0305 ± 0.003	0.136 ± 0.014
3 mM Mn(III)-tartrate	UO_2 and TcO_2	0.0141 ± 0.002	0.120 ± 0.002

concentration of Mn(III)-citrate, although there was less of an increase with higher concentration than expected. TcO_2 dissolution reached between 60 and 85% and plateaued once the Mn(III)-citrate had been entirely consumed. This indicates that dissolution may continue to proceed further with higher concentrations of Mn(III)-citrate. As discussed above with UO_2, this enhanced technetium dissolution could also be due to radical species formed by the electron exchange between Mn(III) and citrate, as opposed to direct oxidation of Tc from Mn(III). However, negligible variation in the extent of TcO_2 oxidation was evident across pH 8 and 10, despite a greater amount of Mn(III) loss at pH 10, indicating the possibility of a higher amount of radicals formed at this pH. Similarly, the redox threshold necessary to oxidize TcO_2 is higher at pH 8 than at pH 10 based on Pourbaix diagrams (SI), but this did not seem to hinder oxidation at pH 8 (Fig. 4).

Trials with Mn(III)-tartrate also had considerable dissolution at both pH 8 and 10. Unlike with Mn(III)-citrate, there was a more significant difference between the two pH values for Mn(III)-tartrate. The trials at pH 8 had significantly more dissolution than at pH 10. This further aligns with the findings of the Job plots which indicate that the presence of additional tartrate ligands at elevated pH may result in steric hindrance, reducing the ability of the complex to interact with and oxidize the TcO_2 surface. As with Mn(III)-citrate, there was significantly greater dissolution for the higher concentration of Mn(III)-tartrate. Overall dissolution of TcO_2 also ranged much more widely here than it did for Mn(III)-citrate, with dissolution ranging between 25 and 90% and once again plateauing once the Mn(III)-tartrate had been entirely consumed in most cases.

In comparison to the TcO_2 dissolution with Mn(III)-pyrophosphate previously studied by Stanberry, *et al.* there was a similar percentage of dissolution achieved in most cases.[34] It is important to note, however, that dissolution occurred much faster with Mn(III)-pyrophosphate than it did with Mn(III)-citrate or Mn(III)-tartrate. The former saw a plateau within a matter of hours while the latter saw a plateau after a week or more. This indicates that while all three of these ligand complexes are able to oxidize TcO_2, and are thus a threat to technetium remobilization, Mn(III)-pyrophosphate does so on a much faster timescale. Additional literature has shown other environmentally relevant species, including manganese oxides, can contribute to TcO_2 oxidation and remobilization.[52,53]

3.4 UO_2 and TcO_2 combined dissolution

A combined dissolution trial of UO_2 and TcO_2 was conducted to assess potential competitive interactions between uranium and technetium dissolution when exposed to Mn(III)-ligands simultaneously (Fig. 5). Uranium dissolution stayed comparable to dissolution in the absence of TcO_2, although a higher amount of dissolution was noted with Mn(III)-citrate than with Mn(III)-tartrate. Technetium dissolution was also comparable to results in the absence of UO_2. These results are summarized in Table 1. In general, the combined presence of UO_2 and TcO_2 caused slightly increased dissolution of both radionuclides with Mn(III)-citrate and slightly decreased dissolution with Mn(III)-tartrate, however the magnitude of this dissolution remained relatively constant for each species. These results suggest that there is minimal competition between the oxidation of these species, and that technetium is more readily oxidized by Mn(III)-ligand complexes than UO_2, likely due to the higher oxidation resistance of the synthesized UO_2 particles as discussed previously. Complete Mn(III) loss was seen with UO_2 and TcO_2 present, consistent with previous results from the TcO_2 dissolution trials, likely due to residual sulfides in the technetium synthesis as discussed previously.

4. Conclusions

This study investigated the redox behavior of environmentally relevant Mn(III)-citrate and Mn(III)-tartrate in promoting the oxidation of UO_2 and TcO_2, given the significant influence of oxidation state on the solubility and environmental mobility of these radionuclides. Overall, UO_2 was resistant to oxidation by both of these Mn(III)-ligand complexes, highlighting the selective and ligand-dependent nature of Mn(III)-mediated redox processes under anoxic conditions. These differences are attributed to a combination of radical formation during Mn(III) oxidation of citrate or tartrate, pH dependent oxidation potentials of UO_2 and TcO_2, and variations in Mn(III)-ligand speciation. Mn(III)-citrate forms predominantly 1 : 1 complexes, while Mn(III)-tartrate forms multi-ligand complexes whose pH dependent structure may introduce steric constraints that influence redox activity. Technetium oxidation occurred more readily than uranium across the investigated conditions, underscoring fundamental differences in how Mn(III)-ligand complexes interact with redox sensitive radionuclide phases. For Mn(III)-tartrate, however, oxidation was significantly lower at pH 10, likely due to the radical species and steric hindrance previously mentioned, suggesting that Mn(III) decay pathways compete with direct mineral oxidation. These findings demonstrate that Mn(III)-citrate and Mn(III)-tartrate can oxidize UO_2 and TcO_2 to varying extents, depending on the pH and

Mn(III)-ligand concentration. Further analysis of the Mn(III)-citrate and Mn(III)-tartrate complexes would be beneficial to determine the oxidation potential of these complexes. Altogether, environmental conditions that facilitate the formation of Mn(III)-ligand complexes should be considered in predictive models describing the stability and mobility of redox-sensitive radionuclides and other contaminants. These results expand the recognized role of Mn(III) from strongly chelated complexes or from mineral phases to include environmentally abundant organic ligands capable of mediating radionuclide oxidation under anoxic conditions.

Conflicts of interest

There are no conflicts to declare.

Data availability

Data for this article, including raw UV-vis and NMR data, as well as origin files that contain calculations are available at Harvard Dataverse at https://doi.org/10.7910/DVN/AFZYNQ

Supplementary information (SI) is available. See DOI: https://doi.org/10.1039/d5va00264h.

Acknowledgements

The authors acknowledge the Materials Characterization Facility (MCF), Advanced Materials Processing and Analysis Center (AMPC) at the University of Central Florida for the use of XRD. The authors also acknowledge the Santra Research Group at the University of Central Florida for the use of SEM.

References

1 G. Gee, M. Oostrom, M. Freshley, M. Rockhold and J. Zachara, Hanford Site Vadose-Zone Studies: An Overview, *Vadose Zone J.*, 2007, **6**, 899–905, DOI: 10.2136/vzj2006.0179.

2 J. Icenhower, N. Qafoku, W. Martin and J. Zachara, The Geochemistry of Technetium: A Summary of the Behavior of an Artificial Element in the Natural, *Environment*, 2008, DOI: 10.2172/1010487.

3 R. E. Gephart, *Hanford; Conversation about Nuclear Waste and Cleanup*, Battelle Press, 2003.

4 R. E. Gephart, A short history of waste management at the Hanford Site, *Phys. Chem. Earth, Parts A/B/C*, 2010, **35**(6), 298–306, DOI: 10.1016/j.pce.2010.03.032.

5 D. J. Washenfelder, and J. M. Johnson Hanford Double-Shell Tank AY-102 Radioactive Waste Leak Investigation Update – 15302, in *Conference: WM2015 Waste Management Symposium 03/15/2015*, Phoenix, AZ, United States, 2014.

6 C. L. Girardot, D. G. Harlow, J. G. Field, J. S. Schofield, T. J. Venetz, D. J. Washenfelder, and J. M. Johnson, Hanford single-shell tanks leak causes and locations - 15509. United States, 01, 2015; Research Org.: WM Symposia, Inc., PO Box 27646, 85285-7646 Tempe, AZ (United States), Conference: WM2015: Annual Waste Management Symposium, Phoenix, AZ (United States), 15-19 Mar 2015; Other Information: Country of input: France; 10 refs.; available online at: https://archive.wmsym.org/2015/index.html.

7 B. J. Wiersma, The Performance of Underground Radioactive Waste Storage Tanks at the Savannah River Site: A 60-Year Historical Perspective, *JOM*, 2014, **66**(3), 471–490, DOI: 10.1007/s11837-014-0870-x.

8 R. G. Riley, and J. M. Zachara, *Chemical Contaminants on DOE Lands and Selection of Contaminant Mixtures for Subsurface Science Research*, United States, 1992, DOI: 10.2172/10147081.

9 J. G. Reynolds, G. A. Cooke, J. S. Page and R. W. Warrant, Uranium-bearing phases in Hanford nuclear waste, *J. Radioanal. Nucl. Chem.*, 2018, **316**(1), 289–299, DOI: 10.1007/s10967-018-5724-5.

10 T. E. Eriksen, D. W. Shoesmith and M. Jonsson, Radiation induced dissolution of U_{O2} based nuclear fuel – A critical review of predictive modelling approaches, *J. Nucl. Mater.*, 2012, **420**(1), 409–423, DOI: 10.1016/j.jnucmat.2011.10.027.

11 A. Abdelouas, W. Lutze, and H. E. Nuttall, 9. Uranium Contamination in the Subsurface: Characterization and Remediation, in *Uranium*, ed. C. B. Peter, and J. F. Robert, De Gruyter, 1999, pp. 433–474.

12 B. D. Hanson, B. McNamara, E. C. Buck, J. I. Friese, E. Jenson, K. Krupka and B. W. Arey, Corrosion of commercial spent nuclear fuel. 1. Formation of studtite and metastudtite, *Radiochim. Acta*, 2005, **93**(3), 159–168, DOI: 10.1524/ract.93.3.159.61613.

13 M. Barger and C. M. Koretsky, The influence of citric acid, EDTA, and fulvic acid on U(VI) sorption onto kaolinite, *Appl. Geochem.*, 2011, **26**, S158–S161, DOI: 10.1016/j.apgeochem.2011.03.092.

14 J. C. Lozano, P. Blanco Rodríguez, F. Vera Tomé and C. P. Calvo, Enhancing uranium solubilization in soils by citrate, EDTA, and EDDS chelating amendments, *J. Hazard. Mater.*, 2011, **198**, 224–231, DOI: 10.1016/j.jhazmat.2011.10.026.

15 L. Chen, J. Liu, W. Zhang, J. Zhou, D. Luo and Z. Li, Uranium (U) source, speciation, uptake, toxicity and bioremediation strategies in soil-plant system: A review, *J. Hazard. Mater.*, 2021, **413**, 125319, DOI: 10.1016/j.jhazmat.2021.125319.

16 S. Akash, B. Sivaprakash, V. C. V. Raja, N. Rajamohan and G. Muthusamy, Remediation techniques for uranium removal from polluted environment – Review on methods, mechanism and toxicology, *Environ. Pollut.*, 2022, **302**, 119068, DOI: 10.1016/j.envpol.2022.119068.

17 T. E. Payne and T. D. Waite, Uranium adsorption – a review of progress from qualitative understanding to advanced model development, *Radiochim. Acta*, 2022, **110**(6–9), 549–559, DOI: 10.1515/ract-2022-0003.

18 U. Becker, and R. C. Ewing, *Actinide Incorporation and Radiation Effects in U(VI) Solids Actinide Sorption and Reduction on Sulfides, Oxides, and Clay Minerals Photoexcitation of Mn-Oxide Minerals and Actinide Metal-Organic Frameworks for Catalysis of Actinyl Complexes and Nanoclusters. Final Report*; DOE-UMICH-15783-1; TRN: US2104883; United States, 2019, DOI: 10.2172/1615667.

19 S. A. Cumberland, G. Douglas, K. Grice and J. W. Moreau, Uranium mobility in organic matter-rich sediments: A review of geological and geochemical processes, *Earth-Sci. Rev.*, 2016, **159**, 160–185, DOI: 10.1016/j.earscirev.2016.05.010.

20 I. Grenthe, J. Fuger, R. J. Lemire, A. B. Muller, C. Ngueyn-Trung Cregu, and H. Wanner, *Chemical Thermodynamics of Uranium*, Elsevier Science Publishers, 1992, vol. 1.

21 D. Langmuir, Uranium solution-mineral equilibria at low temperatures with applications to sedimentary ore deposits, *Geochim. Cosmochim. Acta*, 1978, **42**, 547–569, DOI: 10.1016/0016-7037(78)90001-7.

22 W.-M. Wu, J. Carley, T. Gentry, M. A. Ginder-Vogel, M. Fienen, T. Mehlhorn, H. Yan, S. Caroll, M. N. Pace, J. Nyman, *et al.*, Pilot-Scale in Situ Bioremedation of Uranium in a Highly Contaminated Aquifer. 2. Reduction of U(VI) and Geochemical Control of U(VI) Bioavailability, *Environ. Sci. Technol.*, 2006, **40**(12), 3986–3995, DOI: 10.1021/es051960u.

23 R. T. Anderson, H. A. Vrionis, I. Ortiz-Bernad, C. T. Resch, P. E. Long, R. Dayvault, K. Karp, S. Marutzky, D. R. Metzler, A. Peacock, *et al.*, Stimulating the In Situ Activity of Geobacter Species to Remove Uranium from the Groundwater of a Uranium-Contaminated Aquifer, *Appl. Environ. Microbiol.*, 2003, **69**(10), 5884–5891, DOI: 10.1128/AEM.69.10.5884-5891.2003.

24 C. L. Thorpe, C. Boothman, J. R. Lloyd, G. T. W. Law, N. D. Bryan, N. Atherton, F. R. Livens and K. Morris, The interactions of strontium and technetium with Fe(II) bearing biominerals: Implications for bioremediation of radioactively contaminated land, *Appl. Geochem.*, 2014, **40**, 135–143, DOI: 10.1016/j.apgeochem.2013.11.005.

25 C. Bruggeman, A. Maes and J. Vancluysen, The identification of FeS_2 as a sorption sink for Tc(IV), *Phys. Chem. Earth, Parts A/B/C*, 2007, **32**(8), 573–580, DOI: 10.1016/j.pce.2005.12.006.

26 I. Alliot, C. Alliot, P. Vitorge and M. Fattahi, Speciation of Technetium(IV) in Bicarbonate Media, *Environ. Sci. Technol.*, 2009, **43**(24), 9174–9182, DOI: 10.1021/es9021443.

27 D. Cui and T. E. Eriksen, Reduction of Pertechnetate in Solution by Heterogeneous Electron Transfer from Fe(II)-Containing Geological Material, *Environ. Sci. Technol.*, 1996, **30**(7), 2263–2269, DOI: 10.1021/es950627v.

28 J. K. Fredrickson, J. M. Zachara, D. W. Kennedy, R. K. Kukkadapu, J. P. McKinley, S. M. Heald, C. Liu and A. E. Plymale, Reduction of TcO_4^- by sediment-associated biogenic Fe(II)1 1Associate editor: J. B. Fein, *Geochim. Cosmochim. Acta*, 2004, **68**(15), 3171–3187, DOI: 10.1016/j.gca.2003.10.024.

29 M. J. Truex, J. E. Szecsody, L. Zhong, and N. Qafoku, *Gas-phase Treatment of Technetium in the Vadose Zone at the Hanford Site Central Plateau*, 2014, DOI: 10.2172/1170497.

30 C. I. Pearce, R. C. Moore, J. W. Morad, R. M. Asmussen, S. Chatterjee, A. R. Lawter, T. G. Levitskaia, J. J. Neeway, N. P. Qafoku, M. J. Rigali, *et al.*, Technetium immobilization by materials through sorption and redox-driven processes: A literature review, *Sci. Total Environ.*, 2020, **716**, 132849, DOI: 10.1016/j.scitotenv.2019.06.195.

31 I. Szlamkowicz, J. Stanberry, K. Lugo, Z. Murphy, M. Ruiz Garcia, L. Hunley, N. P. Qafoku and V. Anagnostopoulos, Role of Manganese Oxides in Controlling Subsurface Metals and Radionuclides Mobility: A Review, *ACS Earth Space Chem.*, 2023, **7**(1), 1–10, DOI: 10.1021/acsearthspacechem.2c00113.

32 J. Huang and H. Zhang, Redox reactions of iron and manganese oxides in complex systems, *Front. Environ. Sci. Eng.*, 2020, **14**(5), 76, DOI: 10.1007/s11783-020-1255-8.

33 J. E. Amonette, Iron Redox Chemistry of Clays and Oxides: Environmental Applications, in *Electrochemical Properties of Clays*, Clay Minerals Society, 2002, vol. 10, p. 0, DOI: 10.1346/CMS-WLS-10.3.

34 J. Stanberry, K. Morgan, I. Russell, Z. Ronchetti, T. Carroll and V. Anagnostopoulos, Oxidation and Mobilization of Tc-99 Reduced Phases by a Mn(III)–Pyrophosphate Aqueous Complex under Anoxic Conditions: Implications for Remediation of a Risk-Driving Radionuclide, *ACS Earth Space Chem.*, 2025, **9**(2), 277–287, DOI: 10.1021/acsearthspacechem.4c00274.

35 Z. Wang, W. Xiong, B. M. Tebo and D. E. Giammar, Oxidative UO_2 Dissolution Induced by Soluble Mn(III), *Environ. Sci. Technol.*, 2014, **48**(1), 289–298, DOI: 10.1021/es4037308.

36 K. S. Yamaguchi and D. T. Sawyer, The Redox Chemistry of Manganese(III) and -(IV) Complexes, *Isr. J. Chem.*, 1985, **25**(2), 164–176, DOI: 10.1002/ijch.198500026.

37 F. Li, H. Yin, T. Zhu and W. Zhuang, Understanding the role of manganese oxides in retaining harmful metals: Insights into oxidation and adsorption mechanisms at microstructure level, *Eco-Environ. & Health*, 2024, **3**(1), 89–106, DOI: 10.1016/j.eehl.2024.01.002.

38 S. M. Webb, G. J. Dick, J. R. Bargar and B. M. Tebo, Evidence for the presence of Mn(III) intermediates in the bacterial oxidation of Mn(II), *Proc. Natl. Acad. Sci. U. S. A.*, 2005, **102**(15), 5558–5563, DOI: 10.1073/pnas.0409119102.

39 J. K. Klewicki and J. J. Morgan, Kinetic Behavior of Mn(III) Complexes of Pyrophosphate, EDTA, and Citrate, *Environ. Sci. Technol.*, 1998, **32**(19), 2916–2922, DOI: 10.1021/es980308e.

40 M. Ruiz-Garcia, M. Richards, G. Ballerini Ribeiro Gomes and V. Anagnostopoulos, PbO_2 reductive dissolution by dissolved Mn(III) in the presence of low molecular weight organic acids and humic acid, *Environ. Sci. Pollut. Res.*, 2024, **31**(12), 18540–18548, DOI: 10.1007/s11356-024-32319-9.

41 R. E. Trouwborst, B. G. Clement, B. M. Tebo, B. T. Glazer and G. W. Luther, Soluble Mn (III) in suboxic zones, *Science*, 2006, **313**(5795), 1955–1957, DOI: 10.1126/science.1132876.

42 R. Adeleke, C. Nwangburuka and B. Oboirien, Origins, roles and fate of organic acids in soils: A review, *S. Afr. J. Bot.*, 2017, **108**, 393–406, DOI: 10.1016/j.sajb.2016.09.002.

43 A. Topolski, Insight into the degradation of a manganese(III)-citrate complex in aqueous solutions, *Chem. Pap.*, 2011, **65**(3), 389–392, DOI: 10.2478/s11696-010-0101-z.

44 H. Pan, F. Li, R. Zhang, Y. Liu, J. Li, T. Wu, A. Li and H. Zhou, Superoxide mediated Mn(II) oxidation of an alkali-tolerant

bacterium Pseudorhizobium flavum MXJ-1, *J. Environ. Sci.*, 2025, **160**, 82–92, DOI: 10.1016/j.jes.2025.03.051.

45 M. B. Sears, J. M. Giaquinto, W. H. Griest, R. T. Pack, T. Ross, and R. L. Schenley, *Sampling and Analysis of Inactive Radioactive Waste Tanks W-17, W-18, WC-5, WC-6, WC-8 and WC-11 through WC-14 at ORNL; TM-13017*, Oak Ridge National Laboratory, 1995, https://www.osti.gov/servlets/purl/207660.

46 Y. Sumra, S. Payam and I. Zainah, The pH of Cement-based Materials: A Review, *J. Wuhan Univ. Technol., Mater. Sci. Ed.*, 2020, **35**(5), 908–924, DOI: 10.1007/s11595-020-2337-y.

47 J. E. Kostka, G. W. Luther and K. H. Nealson, Chemical and biological reduction of Mn (III)-pyrophosphate complexes: Potential importance of dissolved Mn (III) as an environmental oxidant, *Geochim. Cosmochim. Acta*, 1995, **59**(5), 885–894, DOI: 10.1016/0016-7037(95)00007-0.

48 Q. Yan, Y. Mao, X. Zhou, J. Liang, M. Ye and S. Peng, Synthesis of UO_2 nanocrystals with good oxidation resistance in water at room temperature, *J. Nucl. Mater.*, 2018, **512**, 417–422, DOI: 10.1016/j.jnucmat.2018.10.005.

49 M. R. Jones, G. W. Luther, A. Mucci and B. M. Tebo, Concentrations of reactive Mn(III)-L and MnO_2 in estuarine and marine waters determined using spectrophotometry and the leuco base, leucoberbelin blue, *Talanta*, 2019, **200**, 91–99, DOI: 10.1016/j.talanta.2019.03.026.

50 M. Ginder-Vogel, C. S. Criddle and S. Fendorf, Thermodynamic Constraints on the Oxidation of Biogenic UO_2 by Fe(III) (Hydr)oxides, *Environ. Sci. Technol.*, 2006, **40**(11), 3544–3550, DOI: 10.1021/es052305p.

51 Z. Wang, S.-W. Lee, P. Kapoor, B. M. Tebo and D. E. Giammar, Uraninite oxidation and dissolution induced by manganese oxide: A redox reaction between two insoluble minerals, *Geochim. Cosmochim. Acta*, 2013, **100**, 24–40, DOI: 10.1016/j.gca.2012.09.053.

52 J. Stanberry, I. Szlamkowicz, D. Magno, L. Shultz and V. Anagnostopoulos, Oxidative dissolution of TcO_2 by Mn(III) minerals under anaerobic conditions: Implications on technetium-99 remediation, *Appl. Geochem.*, 2021, **127**, DOI: 10.1016/j.apgeochem.2020.104858.

53 J. Stanberry, I. Szlamkowicz, L. R. Purdy and V. Anagnostopoulos, TcO_2 oxidative dissolution by birnessite under anaerobic conditions: a solid–solid redox reaction impacting the environmental mobility of Tc-99, *Environ. Sci.: Processes Impacts*, 2021, **23**(6), 844–854, DOI: 10.1039/D1EM00011J.